Controlled Nutrient Delivery to Pancreatic Islets Using Polydopamine Coated Mesoporous Silica Nanoparticles

Mehdi Razavi[1,2,3], Rosita Primavera[1], Bhavesh D Kevadiya[1], Jing Wang[1], Mujib Ullah[1], Peter Buchwald[4] & Avnesh S Thakor[1*]

[1]Interventional Regenerative Medicine and Imaging Laboratory, Stanford University School of Medicine, Department of Radiology, Palo Alto, California 94304, USA

[2]Biionix[TM] (Bionic Materials, Implants & Interfaces) Cluster, Department of Internal Medicine, College of Medicine, University of Central Florida, Orlando, Florida 32827, USA

[3]Department of Materials Science & Engineering, University of Central Florida, Orlando, FL 32816, USA

[4]Diabetes Research Institute, Miller School of Medicine, University of Miami, Miami, Florida 33136, USA

[*]A. S. Thakor is the corresponding author of this work. e-mail: asthakor@stanford.edu

MATERIALS AND METHODS

1. PDG-MSNPs Synthesis

MSNPs were synthesized employing a modified Stöber method using tetraethyl orthosilicate (TEOS) in the presence of cetyl trimethylammonium bromide (CTAB) as structure directing agent.[1] In brief, CTAB (1 g; Fischer Scientific, USA), milliQ H_2O (480 mL) and sodium hydroxide (2 M, 3.5 mL; Fischer Scientific, USA) were stirred and heated to 80°C. Next, TEOS (5 mL; 98%, Fischer Scientific, USA) was added dropwise at 0.25 mL/min to create a white suspension. The obtained white suspension was then magnetically stirred (600 rpm) for further 2 h at 95°C. The reaction mixture was collected by centrifugation (10,000 g for 15 min at 4°C) and washed 3 times in water and ethanol 95% v/v. The surfactant, CTAB, was removed by ionic exchange using a solution of ammonium nitrate (10 mg/mL, Fischer Scientific, USA) in ethanol 95% v/v under magnetic stirring (250 rpm) for 24 h at room temperature. The nanoparticles were collected by centrifugation (10,000 g for 15 min at 4°C), and washed 3 times with ethanol 95% v/v. Next, glutamine was loaded into the synthesized MSNPs. Specifically, 500 mg of MSNPs were added into 10 mL of glutamine solution (10, 30 and 50 mM in water) and mixed at room temperature for 48 h (see paragraph 5.3). Following, the surface of glutamine-loaded MSNPs (G-MSNPs) was coated using dopamine solution in Tris buffer (10 mM, pH = 8.5).[2] Briefly, 500 mg of G-MSNPs were added into 10 mL of dopamine solutions at different concentrations (0.5, 1, and 2 mg/mL) for 0.5 h or at concentration 0.5 mg/mL for different incubation times (0.5, 1, and 2h). G-MSNPs were mixed with polydopamine solutions (at the concentrations and times previously discussed) in an orbital shaker in the dark. The resultant polydopamine coated glutamine-loaded MSNPs (PDG-MSNPs) were collected by centrifugation (10,000 g for 15 min at 4°C), washed 3 times in phosphate buffered saline (PBS; Gibco, USA) and dried at room temperature overnight. To avoid any reaction of polydopamine with PBS, and G release, during the washing process, we minimized the process of mixing PDG-MSNPs with PBS (<15s).

2. PDG-MSNPs Characterization

The average size and size distribution of MSNPs, G-MSNPs and PDG-MSPs have been analyzed using dynamic light scattering. Samples were diluted with milliQ water (1:50 v/v) to avoid multiscattering phenomena and analyzed at 25°C with a Zetasizer Nano ZS90 (Malvern, UK), equipped with a 4.5 mW laser diode and operating at 670 nm as a light source, and the scattered photons were detected at 173°. A third order cumulative fitting autocorrelation function is applied to measure the average size and the size distribution. The analysis was performed according to the following instrumental setup: (i) a real refractive index of 1.59; (ii) an imaginary refractive index of 0.0; (iii) a medium refractive index of 1.330; (iv) a medium viscosity of 1.0 mPa s; and (v) a medium dielectric constant of 80.4.

X-ray diffraction (XRD) analysis was carried out in 2θ range of 2–80° using a PANalytical Empyrean diffractometer (PANalytical Inc., Westborough, MA, USA) with Cu- Kα radiation (1.5418 Å) at 40 kV, 45 mA setting. A mask of 20 mm and a divergence slit of 1/8° were used on the incident beam path. The powder samples were spread on a low background silicon sample holder and the diffraction data was collected in steps of 0.013° by continuously scanning the source and the solid state PIXcel3D detector with a scan rate of 0.01°/s. Ni-foil Kβ filter was introduced in front of the detector to remove possible spurious peaks originating from Cu-Kβ radiation.

Size of nanoparticles and polydopamine coating were also confirmed using Transmission Electron Microscopy (TEM) (Hitachi H7500 TEM) by adding 2 µL of nanoparticle solution on a copper grid (FCF-

400-CU, Electron Microscopy Sciences–EMS, Hatfield, PA, USA). A Zetasizer Nano ZS90 (Malvern, UK) was used to measure the surface charge (zeta-potential, mV) of uncoated and polydopamine-coated G-MSNPs obtained using different PD coating concentrations (0.5 - 2 mg/mL) and times (0.5 - 2 h). Samples were diluted with milliQ water (1:50 v/v) to avoid multiscattering phenomena and analyzed at 25°C. The measurement was performed by using a Smoluchowski constant F (Ka) of 1.5 as a function of the electrophoretic mobility. Measurements represented the average of three batches (10 runs per measurements).

The pore diameter within the nanoparticles was evaluated using a standard nitrogen absorption Brunauer, Emmett and Teller test. Samples were degassed for 48 h at 350°C before measuring the nitrogen adsorption by using a Micromeritics ASAP 2460 Accelerated Surface Area and Porosimetry System with a smart VacPrep system for degassing. The scan parameters were as follow: p/p0 = 0.02-0.2 Steps 0.02 (9 pts), p/p0 = 0.25-0.8 Steps 0.5 (12 pts) and p/p0 = 0.825-0.995 steps 0.25 (9 pts) followed by returning to p/p0=0.08.

3. Determination of Glutamine Loading and Release from PDG-MSNPs

Glutamine solutions were created at concentrations of 10, 30, and 50mM by dissolving glutamine powder in deionized water. MSNPs (500mg) were then added into the glutamine solutions (10mL) and stirred at room temperature for 48h. At 1, 4, 24, and 48h following the addition of MSNPs (500mg) into glutamine solution, the loading efficiency was calculated by measuring the concentration of glutamine remaining in solution using a Bradford assay,[3] according to Equation 1:

$$Glutamine\ Loading\ (\%) = 100 - \left[\left(\frac{mass\ of\ glutamine\ unloaded\ in\ MSNPs}{tot\ mass\ of\ glutamine}\right)\right] X\ 100 \quad \textbf{(Equation 1)}$$

While, to determine *in vitro* glutamine release from nanoparticles, PDG-MSNPs (500 mg) were dispersed in PBS solution (10 mL, pH = 7.4), under magnetic stirrer at 37°C. At predetermined time points (day 1, 2, 3, 7, 10, and 14), the amount of glutamine released in PBS solution was measured using a Bradford assay.[3]

4. Computational Modeling of Glutamine Delivery to Pancreatic Islets from PDG-MSNPs

To estimate the effects that glutamine released form our PDG-MSNPs can have on the survival and function of islets, we performed computational modeling analysis using an updated version of a previously developed and calibrated quantitative model for avascular pancreatic islets.[4,5] Briefly, the previous model used a total of four concentrations for convective and diffusive mass transport modeling with their corresponding equations (application modes) [glucose, oxygen, and local and released insulin ($c_{glucose}$, c_{oxygen}, $c_{local\ insulin}$, and $c_{released\ insulin}$)]. Now, we have added an additional module for the modeling of the mass transport of glutamine ($c_{glutamine}$). As before, diffusion of all species was assumed to be governed by the generic diffusion equation in its non-conservative formulation (incompressible fluid):

$$\frac{\partial c}{\partial t} + \nabla \cdot (-D\nabla c) = R - \mathbf{u} \cdot \nabla c \quad \textbf{(Equation 2)}$$

where c denotes the concentration [mol·m^{-3}], D the diffusion coefficient [m^2·s^{-1}], R the reaction rate [mol·m^{-3}·s^{-1}], $\mathbf{u}$ the velocity field [m·s^{-1}], and ∇ the standard del (nabla) operator ($\nabla \equiv \mathbf{i}\frac{\partial}{\partial x} + \mathbf{j}\frac{\partial}{\partial y} + \mathbf{k}\frac{\partial}{\partial z}$). All consumption and release rates were assumed to follow Hill–type dependence on local concentrations:

$$R = f_H(c) = R_{max}\frac{c^n}{c^n + C_{Hf}^n} \quad \textbf{(Equation 3)}$$

Here, R_{max} denotes the maximum reaction rate [$mol \cdot m^{-3} \cdot s^{-1}$], C_{Hf}, the concentration corresponding to half-maximal response [$mol \cdot m^{-3}$], and n, the Hill slope characterizing the shape of the response. Diffusion coefficients and parameter (R_{max}, C_{Hf}, and n) values used for glucose, oxygen, and insulin are those from the previously developed model,[4] and values for glutamine have been added now. Diffusion coefficients of $D_{glut} = 1.0 \times 10^{-9}$ and 0.33×10^{-9} m^2/s were used for glutamine in aqueous media and islet, respectively. Islets were assumed to have a glutamine consumption rate of 5 nM/day/islet corresponding to 0.033 $M/s/m^3$ per unit volume.[6] Due to the small size of the nanoparticles compared to those of the islets, they were not modelled individually; instead, glutamine release was assumed to be homogeneous in the media surrounding the islets and proportional with the density of nanoparticles present. The sustained-release nanoparticles were assumed to be homogenously dispersed (1,000 nanoparticles per islets in 1 mm^3) with glutamine release rates of 3.6 nM/day/1000 particle resulting in a release rate used in the model of 0.01 $M/m^3/s$ per unit volume (corresponding to release rates measured ~2 weeks after transplantation). As before, the model was implemented in COMSOL Multiphysics (COMSOL Inc., Burlington, MA) and solved as a time-dependent (transient) problem with intermediate time-steps for the solver. The geometry used assumes islets with diameters of 120 and 150 μm cultured with PDG-MSNPs with a ratio of 1:1000 as used in this study. As the model is general and has no size- or geometry related assumptions built into it, it can be used without any additional assumptions. Mesh and boundary conditions used for glucose, oxygen, and insulin, are as described before with symmetry conditions imposed here on the left and right borders (insulin: outflow; oxygen and glucose: fixed concentration on top and bottom). Boundary conditions for glutamine were similar: fixed concentration on top and bottom, symmetry on left and right. The system was assumed to be in an aqueous media at physiological temperature (37°C), extracellular glutamine concentrations of 0.7 mM,[7,8] and a glucose concentration of 8 mM. In a second set of models, a partition coefficient of 5 was assumed between intra- and extracellular domains, which has been built into the model through a special boundary condition using the stiff-spring method as before, and the islets were modeled as a single large cell.

5. *In vitro* Interactions of PDG-MSNPs with Pancreatic Islets

For all *in vitro* experiments, isolated islets were individually counted and manually picked-up under a microscope to achieve a density of 20 islets/well (20 islets in 200 μL of complete medium: RPMI-1640 medium (Gibco, USA) supplemented with 10% fetal bovine serum (FBS; Invitrogen, USA) and 50 U/mL penicillin-50 μg/mL streptomycin (P/S; Invitrogen, USA) were added into 96-well non-adherent tissue culture plates. All the *in vitro* experiments have been performed in quintuplicate (n = 5) using the following experimental groups: Group 1 = islets only (control); Group 2 = islets cultured with glutamine alone at concentrations of 10mM (1.5 mg/mL), 30 mM (4.5 mg/mL), and 50mM (7.5 mg/mL); Group 3 = islets cultured with G-MSNPs (50 mM of glutamine); Group 4 = islets cultured with PDG-MSNPs (50 mM of glutamine) with polydopamine coating concentrations of 0.5, 1, and 2 mg/mL and coating time of 0.5 h; and Group 5 = islets cultured with PDG-MSNPs (50 mM of glutamine)with polydopamine coating times of 0.5, 1, and 2 h and coating concentration of 0.5 mg/mL.

5.1. Mouse Pancreatectomy and Islet Isolation

All mice within this study were treated in accordance with the guidelines approved by the Institutional Animal Care and Use Committee (IACUC) at Stanford University. Animals were housed under conventional conditions having access to food and water *ad libitum*. Pancreatic islets were isolated from C57BL/6 mice (male, 6-8-week-old, Charles River Laboratories, USA), as previously described.[9] In brief,

the common bile duct was cannulated with a 30G needle and the pancreas distended with 3 mL of cold collagenase solution (Fischer Scientific, USA). The pancreas was removed and islets isolated by digesting the pancreas at 37°C for 10 min. The islets were purified using histopaque-density gradients. Islets were then washed with Hank's balanced salt solution (HBSS, Gibco, USA) supplemented with 0.1% bovine serum albumin (BSA, Gibco, USA) before being cultured in complete medium (RPMI (Gibco, USA) supplemented with 10% fetal bovine serum (FBS; Invitrogen, USA) and 50 U/mL penicillin-50 µg/mL streptomycin) within a humidified incubator at 37°C and 5% CO_2.

5.2. Islet Viability

After 7 days of incubation with PDG-MSNPs, the viability of islets was assessed using Live/Dead and 3-(4,5-Dimethylthiazol-2-yl)-2,5-diphenyltetrazolium bromide (MTT) assays. Islets were labeled using fluorescein diacetate (FDA; for live cells (green fluorescence), Thermo Fisher Scientific, USA) and propidium iodide (PI; for dead cells (red fluorescence), Thermo Fisher Scientific, USA) as the Live/Dead staining solution. The culture medium was removed and the Live/Dead staining solution [FDA (75 µL/well) and PI (75 µL/well)] was added and incubated with islets for 20 min at 37°C / 5% CO2. At the end of the incubation time, the staining solution was removed and cells were washed three times with PBS. Finally, the live cell imaging solution (Thermo Fisher Scientific, USA) was added to each well (200 µL/well) before imaging. Images were acquired with a Zeiss LSM710 Confocal Microscope at a magnification of 20X and figures were created with the FIJI software (ImageJ, GNU General Public License). A minimum of 8 islets per experimental group were analyzed using Image-J / FIJI to quantify live and dead fluorescence within islets and the percentage of live islet were presented.

MTT solution (500 µg/mL) was added to each well and incubated at 37°C / 5% CO_2 for 4 h. MTT is converted to an insoluble formazan crystal. Next, 200 µL of DMSO was added to each well and left at 37°C for 10 min to dissolve the formazan crystals. Absorbance was then measured at 570 nm (Tecan, Mannedorf, Swiss). The percentage of cell viability was assessed according to the following equation:

$$Cell\ Viability\ (\%) = \frac{Abs_T}{Abs_C}\ X\ 100 \qquad \textbf{(Equation 4)}$$

where Abs_T is the absorbance of cells treated with PDG-MSNPs or glutamine alone and Abs_C is the absorbance of control cells (islets alone).

5.3. Islet Function

Islets supplemented with PDG-MSNPs were cultured in a humidified incubator under normal conditions (37°C / 5% CO_2 / 20% O_2). After 7 days of incubation with PDG-MSNPs, the ability of islets to secrete insulin was assessed by exposing them to low glucose (i.e. basal conditions) and high glucose (i.e. stimulated conditions) media (200 µL/well). Islets were incubated in Krebs-Ringer Buffer (KRB; Sigma-Aldrich, USA) spiked with 2.8 mM glucose (low) for 2 h followed by 16.7 mM glucose (high) for 2 h at 37°C / 5% CO_2 / 20% O_2. The supernatants were collected at the end of incubation for both basal and stimulated condition and insulin levels were quantified using a mouse insulin ELISA kit (Mercodia Developing Diagnostics, USA). The total insulin content of islets (i.e. 20 islets) was then normalized to present the amount of insulin secreted per islet.

5.4. Islet Protein Expression

To investigate proteins expressed in the islets, heat shock proteins (HSPs) array (R&D Systems, USA) was performed according to the manufacturer's recommendations with little in house modifications. This

test was carried out in two experimental groups. Group 1 = islets only (i.e. control) and Group 2 = islets cultured with PDG-MSNPs with PD coating concentration and time of 0.5 mg/mL and 0.5 h, respectively. Briefly, islets were homogenized in PBS using protease inhibitors cocktail (Sigma-Aldrich, USA), and centrifuged at 10,000 g for 8 min at 4°C. The total protein concentrations of samples (300 µg) were then determined using a bicinchoninic acid (BCA) assay kit (Sigma-Aldrich, USA) and samples (200 µL) with identified protein concentration were added to a membrane spotted with antibodies against HSPs-related proteins. After incubation at 4°C for 24 h, the membranes were treated with streptavidin-horseradish peroxidase (Sigma-Aldrich, USA). Finally, the protein spots were imaged and quantified using an enhanced chemiluminescence detection system (Bio-Rad, USA) with an image analyzer (ChemiDoc, Bio-Rad, USA).

6. *In vivo* Interactions of PDG-MSNPs with pancreatic Islets

6.1. Islet Transplantation

All experiments were approved by the Institutional Animal Care and Use Committee (IACUC) at Stanford University. Male C57BL/6 mice, 6-8 weeks old (Charles River Laboratories, USA), were used as both donors and recipients. All animals were maintained on a 12 h of light and 12 h of dark with *ad libitum* access to food and water. To induce diabetes, each mouse received an intra-peritoneal injection of streptozotocin (STZ) at the dose of 180 mg/kg; this technique is a well-established model for inducing diabetes in rodents and hence for studying islet transplantation[10–13] given that STZ selectively causes destruction of insulin producing β cells within pancreatic islets.[14] Diabetic mice were randomly assigned into 3 experimental groups and each of them have received 175 islets alone or supplemented with glutamine or with PDG-MSNPs under the right kidney capsule. Group 1 = mice transplanted with islets only (n=6; control group); Group 2 = mice transplanted with islets supplemented with glutamine (n=6); Group 3 = mice transplanted with islets supplemented with PDG-MSNPs (50mM of glutamine) (n=6). Furthermore, for Group 2 was used a dosage of glutamine that matched the amount of glutamine used in the case of PDG-MNPs (Group 3). The volume of transplant graft injected under the kidney capsule was same (V = 10µL) for all tested groups include islets only (V = 5µL islet + 5µL PBS), islets + glutamine alone (V = 5µL islet + 5µL glutamine), and islets + PDG-MSNPs (V = 5µL islet + 5µL PDG-MSNPs).

6.2. Metabolic analysis

All metabolic analyses were performed in conscious, restrained mice, at the indicated time points for 30 days. A drop of blood was collected from the tail vein of the mice and the blood glucose measurements were done using a handheld glucometer (Bayer Contour Glucose Meter, USA). Mice were considered normoglycemic when non-fasting blood glucose levels were less than 200 mg/dL. Intraperitoneal glucose tolerance tests (IPGTT) were performed 2 weeks post-transplantation. Specifically, mice were fasted overnight and fasted blood glucose levels were determined before a solution of glucose (2 g/kg) was administered by intra-peritoneal injection. Subsequently, the blood glucose levels were measured each 30 minutes for 2 hours after injection allowing us to calculate the area under the curve (AUC) and blood glucose clearance rate between transplantation groups. At day 30 post-transplantation, mice were euthanized and serum and tissue (i.e. the EFP with or without PDG-MSNPs) samples collected to determine insulin levels (insulin ELISA kit; Mercodia). In addition, the EFP tissue was processed for histological (i.e. fixed in 4% paraformaldehyde, dehydrated with graded ethanol solutions, embedded in paraffin and sliced with a microtome) and/or molecular (i.e. tissues stored at -80°C for subsequent processing to determine levels of cytokines) analyses.

6.3. Histological Analysis

At euthanasia, the kidneys transplanted with islets alone or supplemented with glutamine or with PDG-MSNPs, were harvested, fixed in 4% paraformaldehyde, dehydrated with graded ethanol solutions, embedded in paraffin and sliced with a microtome. The sections were prepared for histological and immunohistochemical (IHC) analyses to determine islet structure and viability (Haemotoxylin and Eosin (H&E) and insulin staining), and evidence of inflammation (H&E and tumor necrosis factor alpha (TNF-α) staining) via standard procedures. The stained sections were then imaged using a NanoZoomer slide scanner 2.0-RS (Hamamatsu, Japan). Results were analyzed with at least 15-20 islets from 5 different sections through the kidney of each animal. In each islet, the percentage surface area occupied by the positive (dark brown) insulin and TNF-α staining (IHC images), and blood vessels (H&E images) were measured using FIJI Image J software, and reported as the percentage of insulin (%/islet), TNF-α (%/islet) and vascularization (%/islet) of islets.[15–17]

6.4. Molecular Analysis

At euthanasia, blood samples were collected to measure serum insulin levels (insulin ELISA kit; Mercodia). The frozen kidney tissue was then homogenized as follow: tissue samples were placed in a homogenization buffer at a ratio of 1 kidney/1mL buffer; the buffer contained a protease inhibitor combination (Sigma Aldrich, USA) including 4-(2-Aminoethyl)benzenesulfonyl fluoride hydrochloride (AEBSF, 2mM), Aprotinin (0.3μM), Bestatin (116μM), trans-Epoxysuccinyl-L-leucylamido(4-guanidino)butane (E-64, 14μM), Leupeptin (1μM) and ethylenediaminetetraacetic acid (EDTA, 1mM) in tissue protein extraction reagent (ThermoFisher Scientific, USA) containing phenylmethylsulfonyl fluoride (PMSF). All homogenized kidney samples were sonicated 3 times for a total of 8s (Branson SLPe) mixed for 45min at 4°C, before then being centrifuged at 15000rpm (for 15min at 4°C). The tissue supernatant was then collected and the insulin content measured (mouse insulin ELISA kit; Mercodia); results were normalized per kidney for each mouse. The level of tissue cytokines was also measured using a mouse multiplex ELISA (eBiosciences/Affymetrix/Fisher). In brief, beads were first added to a 96 well plate and washed (Biotek ELx405). Samples were then added to the plate containing the mixed antibody-linked beads and incubated at room temperature for 1h followed by overnight incubation at 4°C on a plate shaker (500rpm). Biotinylated detection antibody was then added, after which the plates were incubated at room temperature for 75min on the plate shaker (500rpm). Next, the samples were washed and streptavidin-PE added followed by incubation of the plate 30min at room temperature on the plate shaker (500rpm). The plate was then washed and a reading buffer added to all the wells. Finally, a Luminex Flex 3D instrument was used to read the plates with a lower bound of 50 beads per sample per cytokine. Control assay beads (Radix Biosolutions) were added to all wells.

7. Long-Term Biocompatibility of MSNPs

The long-term biocompatibility of our optimized nanoparticles, PDG-MSNPs obtained using a PD coating concentration of 0.5 mg/mL and a coating time of 0.5 h, was evaluated implanting them in two different locations in C57BL/6 healthy mice: the epididymal fat pad and within the subcutaneous tissue of the mice. After 24 weeks, mice were sacrificed and the blood was collected for routine analysis (chemistry, liver and metabolic panels).

8. In Vivo Tracking of MSNPs

To fluorescently label our PDG-MSNPs, we first synthesized a fluorescein isothiocyanate (FITC)-silane precursor. FITC (Sigma Aldrich, 100mg) and 3-aminopropyl triethoxysilane (APTES; sigma Aldrich, 100µL) were first dissolved in ethanol (100mL) and kept at 40°C for 24h. Separately, CTAB (1000mg) was dissolved in deionized water (480ml) contain NaOH (3.5 mL; 2 M). These two solutions were then mixed and heated to 80°C while stirring at 500rpm to obtain the FITC-silane precursor. The FITC-silane precursor solution (10 mL) and TEOS (5 mL) were then mixed and dissolved in water (15mL). Finally, our synthesized PDG-MSNPs were added to the mixture and allowed to react for 24h at room temperature. Labelled PDG-MSNPs called FITC-PDG-MSNPs were then centrifuged and washed three times with ethanol and water. The *in vivo* stability of our FITC-PDG-MSNPs were studied in C57/B6 mice by implanting them (85mg) under the kidney capsule followed by fluorescence imaging using an *in vivo* imaging system (IVIS, Lago optical imaging system) at 500/550 excitation/emission wavelengths. Before implantation, we ensured that our FITC-PDG-MSNPs preserved their fluorescence stability over time by imaging them after incubation in PBS for 5 days. Mice implanted with FITC-PDG-MSNPs were anesthetized and imaged at 1, 5, 9, and 21 days post-implantation.

9. Statistical Analysis

All experiments were performed in n = 5 for *in vitro* or n = 6 for *in vivo*, and results were expressed as mean ± standard error of the mean (SEM). The statistical analysis (Two-way ANOVA post-hoc Tuckey Test or unpaired Student's t-test) is expressed considering any differences statistically significant when $p<0.05$.

RESULTS AND DISCUSSION

Supporting Table 1. Summary of amino acids reported in the literature that can affect islet survival and function.

Glutamine	**Yes**	**Yes**	**Yes**	**Yes**	**Yes**	**Yes**	**Yes**	**Yes**	[6,8,18–20]
Alanine	**Yes**	**Yes**	No	**Yes**	No	No	No	**Yes**	[6,8,18,19]
Cysteine	No	No	**Yes**	No	No	No	No	No	[18]
Tryptophan	**Yes**	**Yes**	No	No	No	No	No	No	[18,21]
Leucine	No	**Yes**	**Yes**	No	No	No	No	No	[18,19]
Methionine	No	No	No	No	No	No	No	No	[18]
Isoleucine	No	**Yes**	No	No	No	No	No	No	[9]
Arginine	No	**Yes**	No	No	No	No	No	No	[9,22]
Lysine	No	**Yes**	No	No	No	No	No	No	[19]
Proline	No	**Yes**	No	No	No	No	No	No	[19]
Homocysteine	No	No	No	No	No	No	No	No	[19]

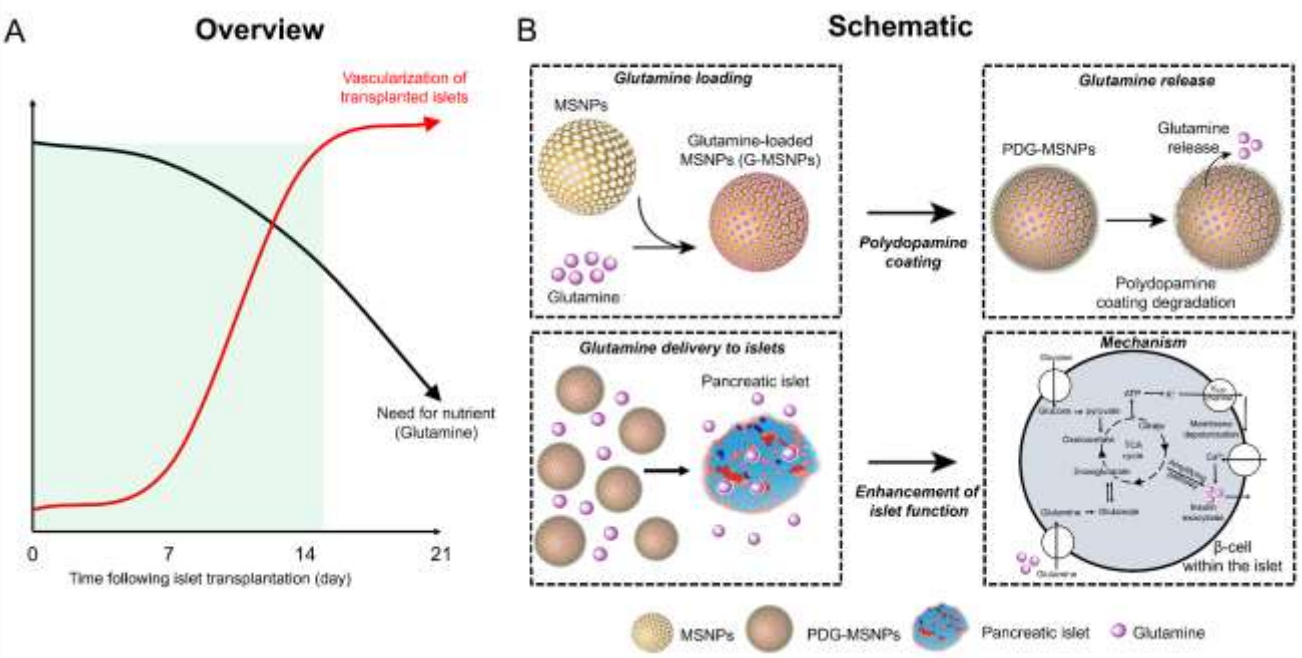

Supporting Figure 1. Role of glutamine and PDG-MSNPs in islets transplantation. A) Overview diagram showing the temporal relationship between the need for nutrients over the first 2 weeks after islet transplantation and the time taken for islets to establish their own blood supply. **B)** Schematic representation showing our nanoscale platform (PDG-MSNP), which can be used to deliver nutrients, such as glutamine, to islets and the mechanism of how glutamine regulates insulin secretion in β-cells within the pancreatic islet.

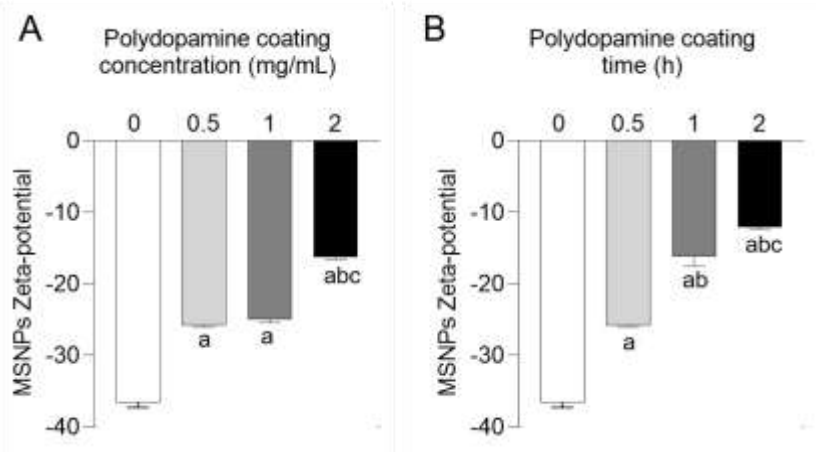

Supporting Figure 2. Surface charge of MSNPs. A, B) The surface charge of uncoated- and PDG-MSNPs obtained using different polydopamine coating concentrations (0, 0.5, 1, 2 mg/mL) (**A**) and times (0, 0.5, 1, 2 h) (**B**). Results are expressed as average ± SEM (n = 5). Statistical analysis (Two-way ANOVA post-hoc Tuckey Test) is expressed as follows, with any differences considered statistically significant when $p<0.05$: (**A**) $^{a}p<0.05$ 0 mg/mL vs. 0.5 mg/mL, 1mg/mL and 2 mg/mL, $^{b}p<0.05$ 0.5 mg/mL vs. 1 mg/mL and 2 mg/mL, $^{c}p<0.05$ 1 mg/mL vs. 2 mg/mL; (**B**) $^{a}p<0.05$ 0 h vs. 0.5 h, 1 h and 2 h, $^{b}p<0.05$ 0.5 h vs. 1 h and 2 h, $^{c}p<0.05$ 1 h vs. 2 h.

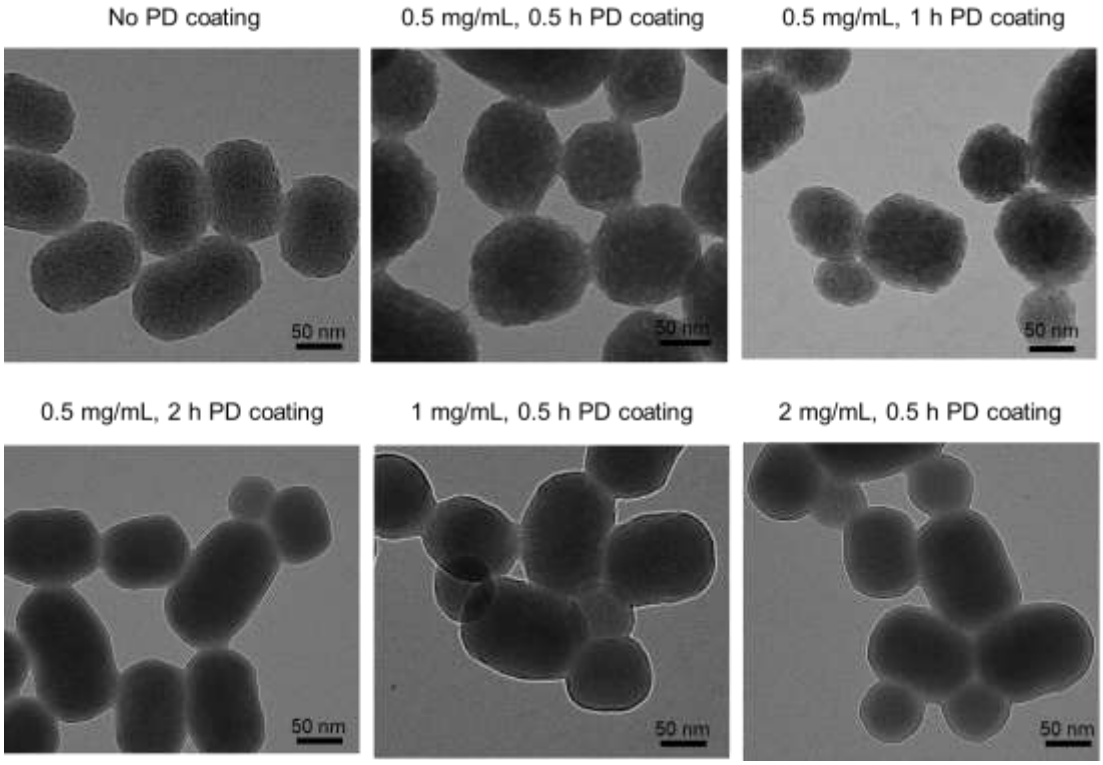

Supporting Figure 3. TEM analysis of MSNPs. Representative TEM images of uncoated- and polydopamine (PD) coated-G-MSNPs obtained using different polydopamine coating concentrations (0, 0.5, 1, 2 mg/mL) and times (0, 0.5, 1, 2 h). Images show a very uneven surface for uncoated G-MSNPs, whereas a smoother surface is observed for polydopamine coated G-MSNPs.

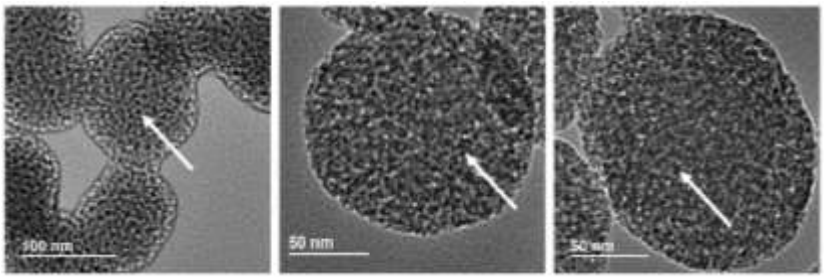

Supporting Figure 4. TEM analysis of MSNPs. Representative TEM images of MSNPs at high magnifications showing the MSNP's pores indicated by white arrows.

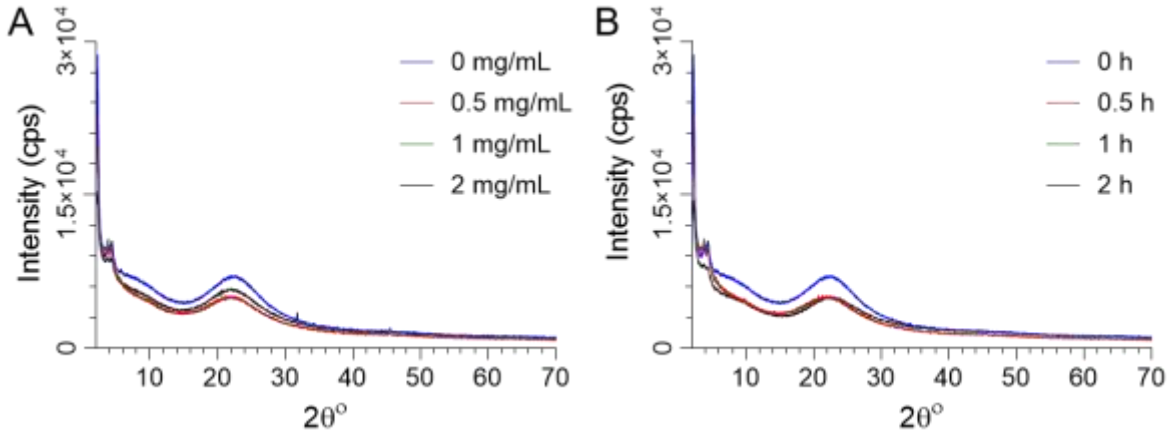

Supporting Figure 5. XRD analysis of MSNPs. XRD analysis of uncoated- and polydopamine coated-G-MSNPs obtained using different polydopamine coating concentrations (0, 0.5, 1, 2 mg/mL) over 0.5 h (**A**) and times (0, 0.5, 1, 2 h) at concentration 0.5 mg/mL (**B**).

A

Surface area measurement		
Specific surface area (m^2/g)	S_{BET}[a]	869.3
Pore volume (cm^3/g)	V_T[b]	0.7
Pore size (nm)	D_{BET}[c]	3.3

[a]Brunauer–Emmer–Teller (BET) surface area.
[b]Single point adsorption total pore volume of pores less than 20.15 nm radius at P/P0 = 0.9500.
[c]Adsorption average pore diameter, obtained from 4 V/A by BET

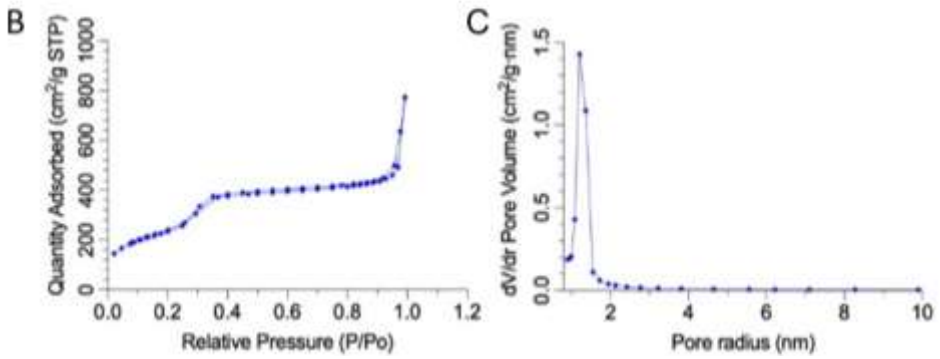

Supporting Figure 6. BET analysis of MSNPs. A) Table showing the surface area measurement of MSNPs, including specific surface area, pore volume and size of uncoated MSNPs. **B, C**) Adsorption/desorption isotherm and average pore radius of MSNPs, respectively.

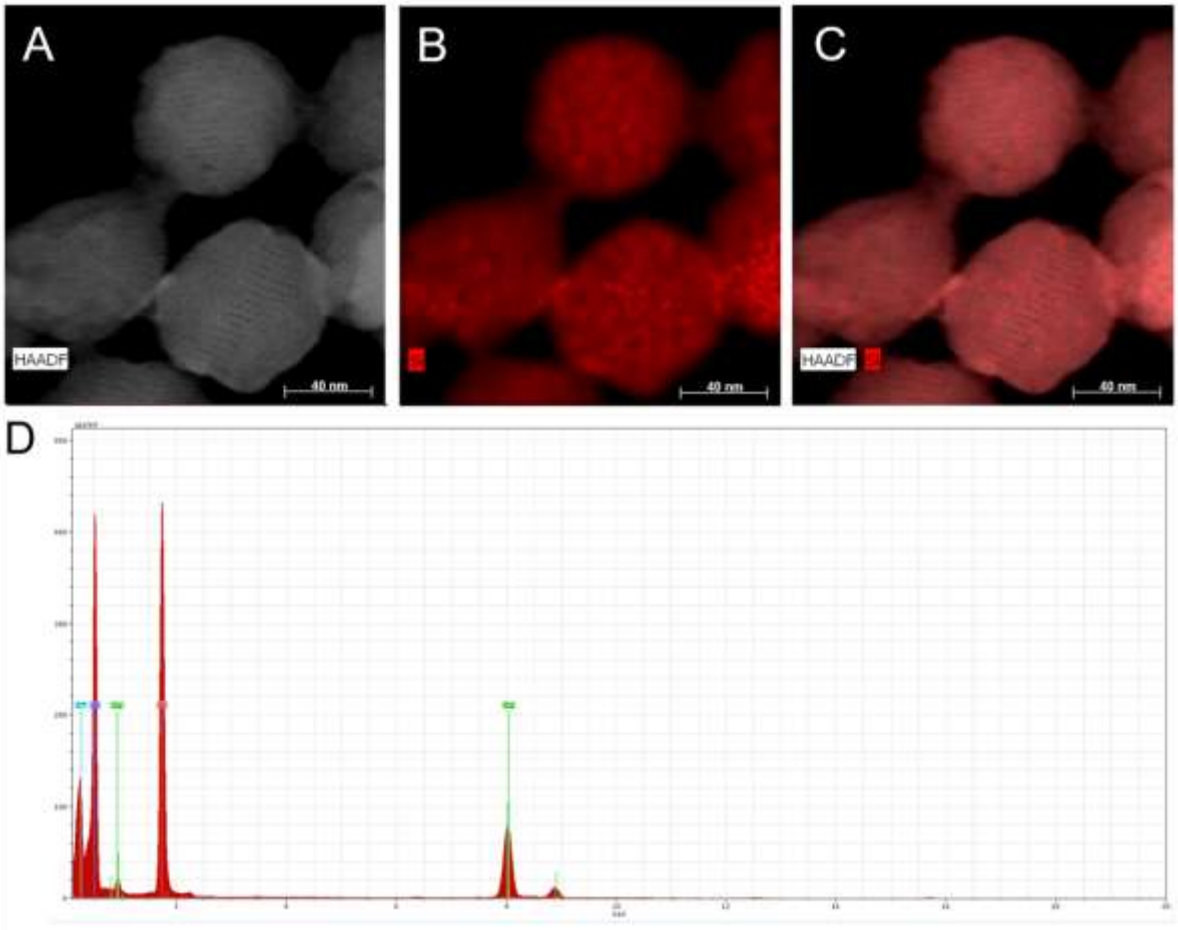

Supporting Figure 7. EDS analysis of MSNPs. A) HADDF image (grey), **B**) corresponding element mapping images of Si, **C**) overlapped image of HAADF and Si mapping, and **D**) energy dispersive X-ray spectrum of uncoated MSNPs. Si and O peaks are related to MSNPs and Cu indicate the copper grid.

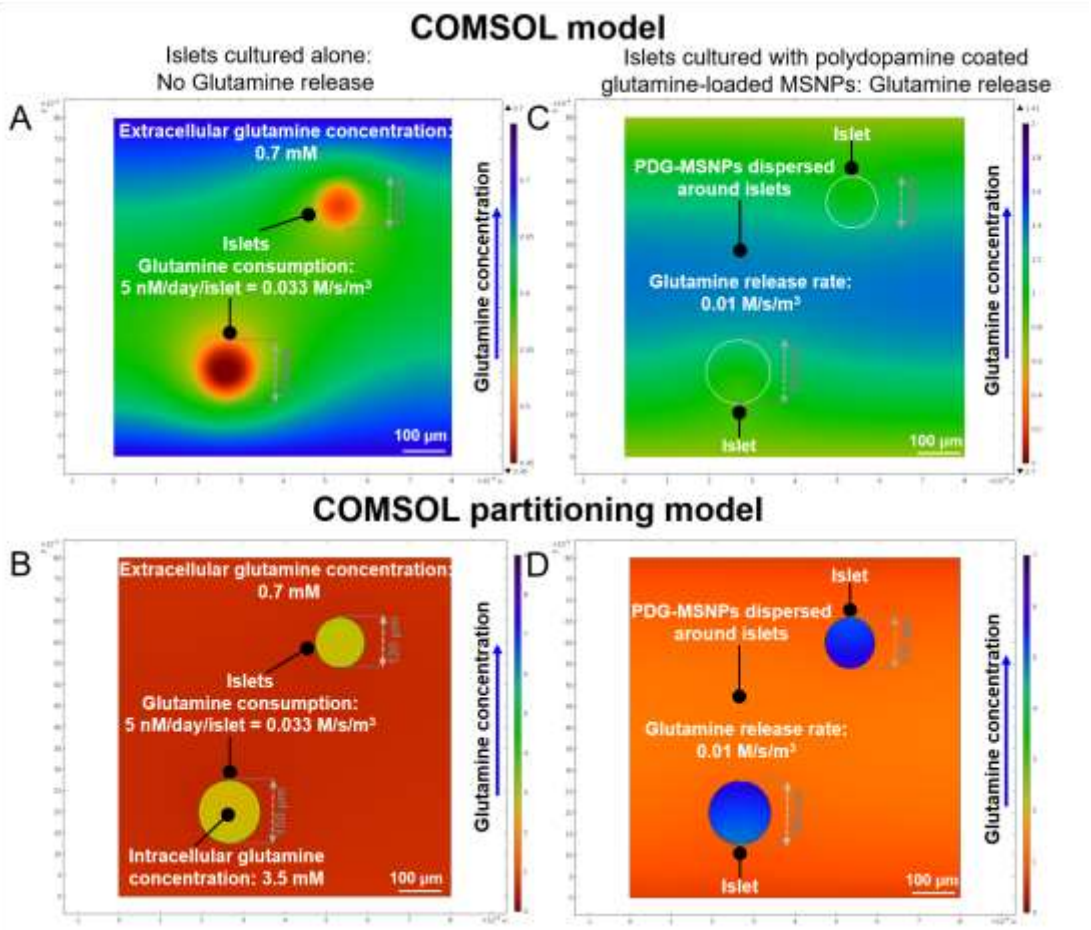

Supporting Figure 8. Computational model-calculated glutamine concentrations. A, B) Glutamine concentrations for two islets with diameter = 120 & 150 µm cultured alone or **C, D**) with PDG-MSNPs that release glutamine (0.01 M/s/m^3) and are assumed to be homogeneously dispersed in the media surrounding the islets. Data are shown in a system assumed to be in an aqueous media at physiological temperature (37°C) with islets having a glutamine consumption of 5 nM/day/islet = 0.033 M/s/m^3, extracellular glutamine concentration of 0.7 mM, and a glucose concentration of 8 mM. Top row (**A**, **C**) shows calculations assuming simple diffusion between intra- and extracellular domains, while bottom row (**B**, **D**) assumes a partition coefficient of 5 between islets and the surrounding media (islets are modeled as essentially a single large cell). Glutamine concentrations are color-coded from blue for high to red for low with red indicating levels that are below the critical concentration of glutamine ($c_{glutamine} < c_{critical}$) for islet survival. Assuming a glutamine consumption rate of 5 nM/day/islet,[6] this result illustrated that the core of islets cultured without glutamine demonstrated both reduced viability and functionality (**A-B**). On the contrary, when islets were cultured with PDG-MSNPs, our computational model showed that glutamine released from PDG-MSNPs (with a glutamine release rate of 0.01 M/s/m^3) improved islet viability and function (**C-D**).

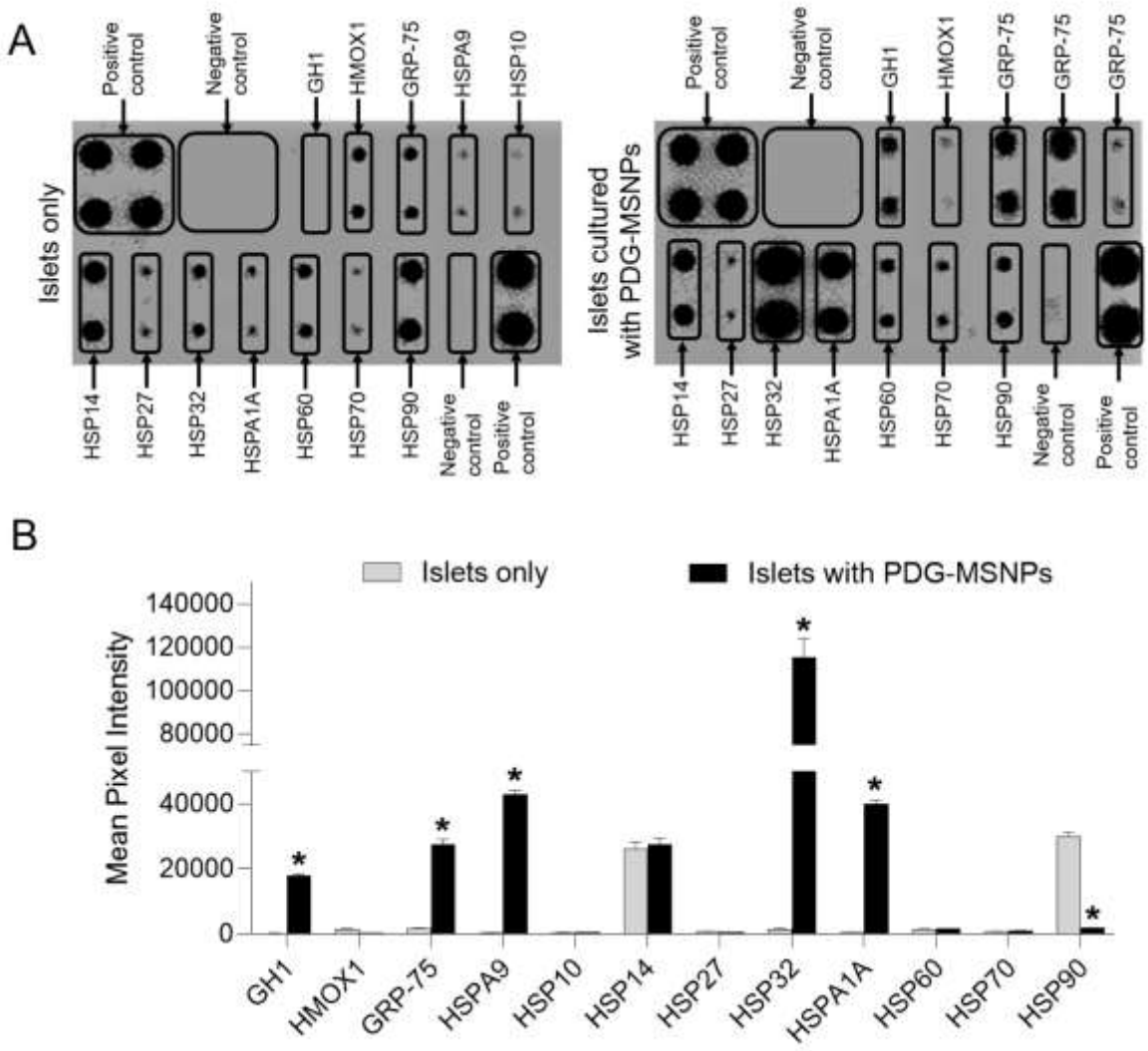

Supporting Figure 9. Islet Protein Expression. Results of protein array analyses show differences in the protein expression of islets cultured with PDG-MSNPs compared to islets only (control). Results are expressed as average ± SEM (n = 5). The statistical analysis (unpaired Student's t-test) is expressed as following, considering any differences statistically significant when $p<0.05$: $^{*}p<0.05$: islets only vs. islets cultured with PDG-MSNPs. The protein array assay assessed that islets supplemented with our optimized PDG-MSNPs (i.e. polydopamine coating concentration of 0.5 mg/mL and time of 0.5 h) had a significantly higher expression of growth hormone 1 (GH1; 18048 ± 994 vs. 225 ± 138 mean pixel density, $p<0.05$), glucose-regulated protein-75 (GRP-75; 27506 ± 2774 vs. 1652 ± 323 mean pixel density, $p<0.05$), heat shock protein A9 (HSPA9; 42954 ± 2133 vs. 375 ± 55 mean pixel density, $p<0.05$), and heat shock protein 32 (HSP32; 115320 ± 15444 vs. 1523 ± 353 mean pixel density, $p<0.05$). On the contrary, the expression of heat shock protein 90 (HSP90) was significantly decreased in islets cultured with PDG-MSNPs compared to islets only (1909 ± 104 vs. 30016 ± 2075 mean pixel density, $p<0.05$). This result shows that, PDG-MSNPs had cytoprotective effects on islets via the induction of growth hormones (GHs), glucose-regulated proteins (GRPs) and heat shock proteins (HSPs) compared to islets cultured with glutamine alone. Islets cultured with PDG-MSNPs highly expressed: GH1 (a growth hormone which regulates immune function),[23] GRP-75 and HSPA9 (members of the HSP70 family which regulate cell growth and survival)[24,25] and HSP32 (a stress-related survival factor that can protect against inflammatory reactions and stress responses).[26] On the contrary,

the expression of HSP90 (a molecular chaperone that promotes both folding and degradation and is associated with apoptosis)[27] was lower in islets cultured with PDG-MSNPs. Our findings are consistent with previous studies which have shown that rat islets supplemented with glutamine will increase the expression of HSP70[20] and mammalian cells supplemented with other amino acids will increase the expression of both HSPs and GRPs.[28] Recent work has also identified HSP32 (heme oxygenase-1) to possess potent proangiogenic properties in addition to well-recognized anti-inflammatory, antioxidant, and antiapoptotic effects.[29] Angiogenic factors, such as VEGF and stromal cell–derived factor-1 (SDF-1), mediate their proangiogenic effects through induction of HSP32, making it an attractive target for therapeutic intervention.[30] Hence, these results shows that PDG-MSNPs have indirect proangiogenic effects on islets via the induction of HSP32.

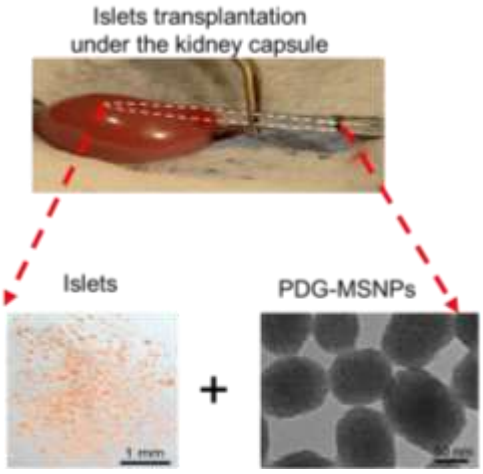

Supporting Figure 10. Islet transplantation performed under the kidney capsule. Photographs of the transplantation procedure of islets (representative image of islets obtained with stereomicroscope after islet isolation procedure) supplemented with PDG-MSNPs (representative TEM image of PDG-MSNPs).

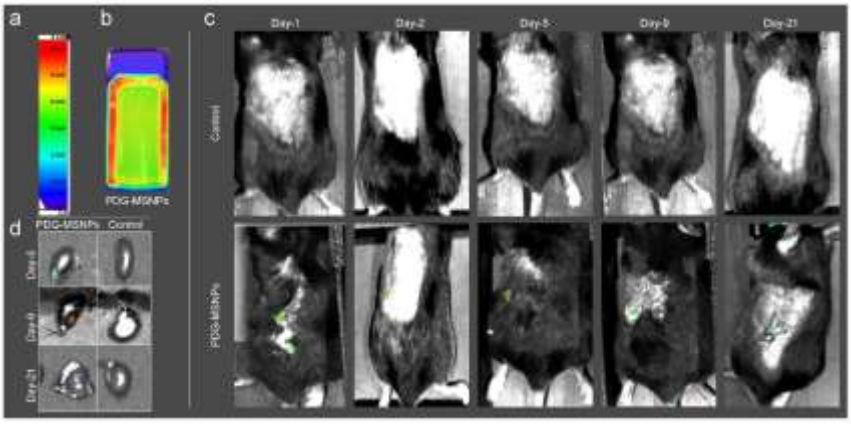

Supporting Figure 11: IVIS imaging of our FITC-PDG-MSNPs: (a) color scale bar demonstrating fluorescent intensity, **(b)** optical image of the fluorescent intensity of our FITC-PDG-MSNPs, **(c)** *in vivo* imaging of C57/B6 mice implanted with our FITC-PDG-MSNPs under their kidney capsule at day 1, 2, 5, 9, and 21 post-implantation, and control non-implanted mice, **(d)** ex vivo imaging of harvested kidneys of mice transplanted with FITC-PDG-MSNPs at day 5, 9, and 21 post-implantation and control non-implanted mice. Following implantation of our FITC-PDG-MSNPs, a persistent fluorescent signal was observed from the kidney at day 1, 2, 5, 9 and 21 post-implantation. This fluorescent signal was observed only in the kidney in which they were implanted and not in any other organ. This result shows the stability of our PDG-MSNPs over the time period required for delivery of nutrients to islets

following transplantation (i.e. 2 weeks). Furthermore, our PDG-MSNPs remain at their site of implantation with no accumulation or redistribution to any other organ.

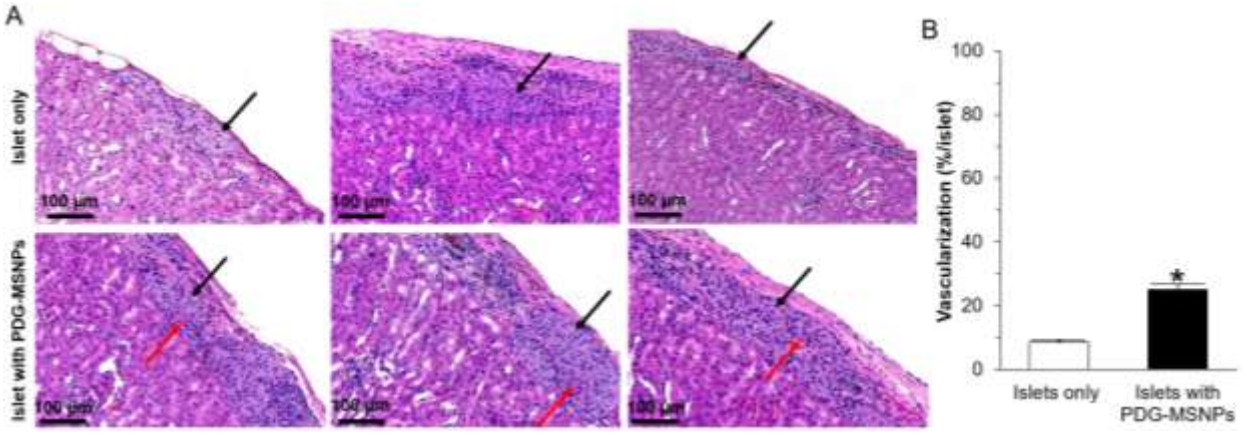

Supporting Figure 12. Histological analysis of kidney tissue after mice sacrifice. A) Representative histological images (H&E staining) of islets transplanted under the kidney capsule (black arrow = islets and red arrow = blood vessels). **B**) Quantification of blood vessels within and around islets supplemented with PDG-MSNPs relative to transplanted islets only (i.e. control). Results are expressed as average ± SEM (n = 6). Statistical analysis (unpaired Student's t-test) is expressed as follows, with any differences considered statistically significant when $p<0.05$: $^{*}p<0.05$: islets only vs. islets with PDG-MSNPs. Using this histological analysis performed on tissue (i.e. kidneys) explanted 30 days post-transplantation, transplanted islets with PDG-MSNPs demonstrated a greater degree of vascularity compared to islets only (25.17 ± 1.45 vs. 8.50 ± 0.53%; $p<0.05$).

Supporting Table 2. Long-term biocompatibility of optimized PDG-MSNPs. Blood metabolic, chemistry, and liver panels from mice that have been implanted with optimized PDG-MSNPs (obtained using a PD coating of 0.5 mg/mL for 0.5 h) for 24 weeks. The normal range for each parameter analyzed is listed in the table. Results are expressed as the average ± SEM (n = 6). We tested the biocompatibility of our nanoparticles in both the epididymal fat pad (a common site for bioscaffold implantation in small animal models which is representative of the omentum in humans) [31,32] as well as the subcutaneous tissue (a site which can be easily accessed in patients and has the potential to be widely adopted as a space for bioscaffold implantation with minimal intervention).[33,34] The blood analysis performed 24 weeks post-implantation confirmed that PDG-MSNPs did not affect the metabolic, chemistry, and liver panels of the mice that have been implanted with particles for 24 weeks. All the values remained within their respective normal range.[35,36] These results show that PDG-MSNPs are biocompatible and cause a minimal change in blood biochemical makers at 6 months following implantation at either site. These findings are in keeping with their ability to be used *in vivo* and hence their potential to be clinically translated.

Test	Mice implanted with PDG-MSNPs	Normal Range
METABOLIC PANEL		
Sodium	150±2	146–151 mmol/L
Chloride	112±1	107–111 mmol/L
Carbon Dioxide	21±2	20–29 mmol/L
Potassium	4.5±0.5	3.0–9.6 mmol/L
Blood Urea Nitrogen	20±3	20.3–24.7 mg/dL
Creatinine	0.14±0.03	0.1–1.1 mg/dL
CHEMISTRY PANEL		
Calcium	9.2±0.2	8.9–9.7 mg/dL
Phosphorus	7.2±0.5	4.2–8.5 mg/dL
T.Protein	4.7±0	4.5–6.5 g/dL
Albumin	2.5±0.1	2.5–2.8 g/dL
LIVER PANEL		
Alkaline Phosphatase	57±5	44–147 IU/L
Aspartate Aminotransferase (AST)	71±41	10–45 U/L
Alanine Aminotransferase (ALT)	70±51	10–35 U/L
Total Bilirubin	0.1±0.05	0–1.0 mg/dL

Supporting Table 3. Statistical analysis for DLS analysis of uncoated- and polydopamine coated-G-MSNPs obtained using different polydopamine coating concentrations (0, 0.5, 1, 2 mg/mL). The p values of < 0.05 (*), < 0.01 (**), < 0.001 (***) and < 0.0001 (****) were considered to be statistically significant, while ns was not statistically significant.

Diameter size (nm)	0 mg/mL vs 0.5 mg/mL	0 mg/mL vs 1mg/mL	0 mg/mL vs 2 mg/mL	0.5 mg/mL vs 1 mg/mL	0.5 mg/mL vs 2 mg/mL	1 mg/mL vs 2 mg/mL
0.40-50.70	ns	ns	ns	ns	ns	ns
58.8	****	****	****	ns	ns	ns
68.1	****	****	****	ns	ns	ns
78.8	****	****	****	***	*	****
91.3	****	****	****	ns	ns	*
106	ns	****	ns	***	ns	*
122	****	ns	**	****	ns	ns
142	****	****	****	**	*	ns
164	****	****	****	ns	ns	ns
190	****	****	****	ns	ns	ns
220	**	****	****	**	ns	*
255	ns	****	ns	***	ns	**
295	ns	ns	ns	ns	ns	ns
342-531	ns	ns	ns	ns	ns	ns

Supporting Table 4. Statistical analysis for DLS analysis of uncoated- and polydopamine coated-G-MSNPs obtained using different polydopamine coating times (0, 0.5, 1, 2 h). The p values of < 0.05 (*), < 0.01 (**), < 0.001 (***) and < 0.0001 (****) were considered to be statistically significant, while ns was not statistically significant.

Diameter size (nm)	0 h vs 0.5 h	0 h vs 1 h	0 h vs 2 h	0.5 h vs 1 h	0.5 h vs 2 h	1 h vs 2 h
0.40-50.70	ns	ns	ns	ns	ns	ns
58.8	****	****	****	ns	ns	ns
68.1	****	****	****	ns	ns	ns
78.8	****	****	****	***	ns	**
91.3	****	****	****	*	*	****
106	ns	ns	****	ns	****	****
122	****	****	ns	ns	****	**
142	****	****	****	*	ns	ns
164	****	****	****	*	ns	3
190	****	****	****	ns	***	****
220	***	**	****	ns	****	****
255	ns	ns	**	ns	ns	*
295	ns	ns	ns	ns	ns	ns
342-531	ns	ns	ns	ns	ns	ns

REFERENCES

(1) Paris, J. L.; Cabanas, M. V.; Manzano, M.; Vallet-Regí, M. Polymer-Grafted Mesoporous Silica Nanoparticles as Ultrasound-Responsive Drug Carriers. *ACS Nano* **2015**, *9* (11), 11023–11033. https://doi.org/10.1021/acsnano.5b04378.

(2) Razavi, M.; Hu, S.; Thakor, A. S. A Collagen Based Cryogel Bioscaffold Coated with Nanostructured Polydopamine as a Platform for Mesenchymal Stem Cell Therapy. *J. Biomed. Mater. Res. - Part A* **2018**, *106* (8), 2213–2228. https://doi.org/10.1002/jbm.a.36428.

(3) Carlsson, N.; Borde, A.; Wölfel, S.; Kerman, B.; Larsson, A. Quantification of Protein Concentration by the Bradford Method in the Presence of Pharmaceutical Polymers. *Anal. Biochem.* **2011**, *411* (1), 116–121. https://doi.org/10.1016/j.ab.2010.12.026.

(4) Buchwald, P. A Local Glucose-and Oxygen Concentration-Based Insulin Secretion Model for Pancreatic Islets. *Theor. Biol. Med. Model.* **2011**, *8* (1). https://doi.org/10.1186/1742-4682-8-20.

(5) Buchwald, P.; Tamayo-Garcia, A.; Manzoli, V.; Tomei, A. A.; Stabler, C. L. Glucose-Stimulated Insulin Release: Parallel Perifusion Studies of Free and Hydrogel Encapsulated Human Pancreatic Islets. *Biotechnol. Bioeng.* **2018**, *115* (1), 232–245. https://doi.org/10.1002/bit.26442.

(6) Dixon, G.; Nolan, J.; McClenaghan, N.; Flatt, P. R.; Newsholme, P. A Comparative Study of Amino Acid Consumption by Rat Islet Cells and the Clonal Beta-Cell Line BRIN-BD11 - The Functional Significance of L-Alanine. *J. Endocrinol.* **2003**, *179* (3), 447–454. https://doi.org/10.1677/joe.0.1790447.

(7) Curi, R.; Lagranha, C. J.; Doi, S. Q.; Sellitti, D. F.; Procopio, J.; Pithon-Curi, T. C.; Corless, M.; Newsholme, P. Molecular Mechanisms of Glutamine Action. *Journal of Cellular Physiology*. 2005, pp 392–401. https://doi.org/10.1002/jcp.20339.

(8) Newsholme, P.; Brennan, L.; Bender, K. Amino Acid Metabolism, β-Cell Function, and Diabetes. *Diabetes* **2006**, *55* (SUPPL. 2). https://doi.org/10.2337/db06-S006.

(9) Neuman, J. C.; Truchan, N. A.; Joseph, J. W.; Kimple, M. E. A Method for Mouse Pancreatic Islet Isolation and Intracellular CAMP Determination. *J. Vis. Exp.* **2014**, No. 88, e50374. https://doi.org/10.3791/50374.

(10) Ren, G.; Rezaee, M.; Razavi, M.; Taysir, A.; Wang, J.; Thakor, A. S. Adipose Tissue-Derived Mesenchymal Stem Cells Rescue the Function of Islets Transplanted in Sub-Therapeutic Numbers via Their Angiogenic Properties. *Cell Tissue Res.* **2019**. https://doi.org/10.1007/s00441-019-02997-w.

(11) Cantarelli, E.; Citro, A.; Marzorati, S.; Melzi, R.; Scavini, M.; Piemonti, L. Murine Animal Models for Preclinical Islet Transplantation: No Model Fits All (Research Purposes). *Islets*. 2013, pp 79–86. https://doi.org/10.4161/isl.24698.

(12) Coronel, M. M.; Geusz, R.; Stabler, C. L. Mitigating Hypoxic Stress on Pancreatic Islets via in Situ Oxygen Generating Biomaterial. *Biomaterials* **2017**, *129*, 139–151. https://doi.org/10.1016/j.biomaterials.2017.03.018.

(13) Pedraza, E.; Coronel, M. M.; Fraker, C. A.; Ricordi, C.; Stabler, C. L. Preventing Hypoxia-Induced Cell Death in Beta Cells and Islets via Hydrolytically Activated, Oxygen-Generating Biomaterials. *Proc. Natl. Acad. Sci.* **2012**, *109* (11), 4245–4250. https://doi.org/10.1073/pnas.1113560109.

(14) Wilson, G. L.; Leiter, E. H. Streptozotocin Interactions with Pancreatic Beta Cells and the Induction of Insulin-Dependent Diabetes. *Curr. Top. Microbiol. Immunol.* **1990**, *156*, 27–54.

(15) Razavi, M.; Zheng, F.; Telichko, A.; Wang, J.; Ren, G.; Dahl, J.; Thakor, A. S. Improving the Function and Engraftment of Transplanted Pancreatic Islets Using Pulsed Focused Ultrasound Therapy. *Sci. Rep.* **2019**, *9* (1). https://doi.org/10.1038/s41598-019-49933-0.

(16) Razavi, M.; Primavera, R.; Kevadiya, B. D.; Wang, J.; Buchwald, P.; Thakor, A. S. A Collagen Based Cryogel Bioscaffold That Generates Oxygen for Islet Transplantation. *Adv. Funct. Mater.* **2020**, *30* (15). https://doi.org/10.1002/adfm.201902463.

(17) Canzano, J. S.; Nasif, L. H.; Butterworth, E. A.; Fu, D. A.; Atkinson, M. A.; Campbell-Thompson, M. Islet Microvasculature Alterations With Loss of Beta-Cells in Patients With Type 1 Diabetes. *J.*

Histochem. Cytochem. **2019**, *67* (1), 41–52. https://doi.org/10.1369/0022155418778546.
(18) Faleo, G.; Russ, H. A.; Wisel, S.; Parent, A. V.; Nguyen, V.; Nair, G. G.; Freise, J. E.; Villanueva, K. E.; Szot, G. L.; Hebrok, M.; et al. Mitigating Ischemic Injury of Stem Cell-Derived Insulin-Producing Cells after Transplant. *Stem Cell Reports* **2017**, *9* (3), 807–819. https://doi.org/10.1016/j.stemcr.2017.07.012.
(19) Liu, Z.; Jeppesen, P. B.; Gregersen, S.; Chen, X.; Hermansen, K. Dose- and Glucose-Dependent Effects of Amino Acids on Insulin Secretion from Isolated Mouse Islets and Clonal INS-1E Beta-Cells. *Rev. Diabet. Stud.* **2008**, *5* (4), 232–244. https://doi.org/10.1900/RDS.2008.5.232.
(20) Jang, H. J.; Kwak, J. H.; Cho, E. Y.; We, Y. M.; Lee, Y. H.; Kim, S. C.; Han, D. J. Glutamine Induces Heat-Shock Protein-70 and Glutathione Expression and Attenuates Ischemic Damage in Rat Islets. *Transplant. Proc.* **2008**, *40* (8), 2581–2584. https://doi.org/10.1016/j.transproceed.2008.08.075.
(21) Lindström, P.; Sehlin, J. Aromatic Amino Acids and Pancreatic Islet Function: A Comparison of l-Tryptophan and l-5-Hydroxytryptophan. *Mol. Cell. Endocrinol.* **1986**, *48* (2–3), 121–126. https://doi.org/10.1016/0303-7207(86)90034-1.
(22) Mullooly, N.; Vernon, W.; Smith, D. M.; Newsholme, P. Elevated Levels of Branched-Chain Amino Acids Have Little Effect on Pancreatic Islet Cells, but l-Arginine Impairs Function through Activation of the Endoplasmic Reticulum Stress Response. *Exp. Physiol.* **2014**. https://doi.org/10.1113/expphysiol.2013.077495.
(23) Millar, D. S.; Lewis, M. D.; Horan, M.; Newsway, V.; Easter, T. E.; Gregory, J. W.; Fryklund, L.; Norin, M.; Crowne, E. C.; Davies, S. J.; et al. Novel Mutations of the Growth Hormone 1 (GH1) Gene Disclosed by Modulation of the Clinical Selection Criteria for Individuals with Short Stature. *Hum. Mutat.* **2003**, *21* (4), 424–440. https://doi.org/10.1002/humu.10168.
(24) Starenki, D.; Hong, S. K.; Lloyd, R. V.; Park, J. I. Mortalin (GRP75/HSPA9) Upregulation Promotes Survival and Proliferation of Medullary Thyroid Carcinoma Cells. *Oncogene* **2015**, *34* (35), 4624–4634. https://doi.org/10.1038/onc.2014.392.
(25) Mizzen, L. A.; Chang, C.; Garrels, J. I.; Welch, W. J. Identification, Characterization, and Purification of Two Mammalian Stres Proteins Present in Mitochondria, Grp 75, a Member of the Hsp 70 Family and Hsp 58, a Homolog of the Bacterial GroEL Protein. *J. Biol. Chem.* **1989**, *264* (34), 20664–20675.
(26) Kondo, R.; Gleixner, K. V.; Mayerhofer, M.; Vales, A.; Gruze, A.; Samorapoompichit, P.; Greish, K.; Krauth, M. T.; Aichberger, K. J.; Pickl, W. F.; et al. Identification of Heat Shock Protein 32 (Hsp32) as a Novel Survival Factor and Therapeutic Target in Neoplastic Mast Cells. *Blood* **2007**. https://doi.org/10.1182/blood-2006-10-054411.
(27) Galea-Lauri, J.; Richardson, A. J.; Latchman, D. S.; Katz, D. R. Increased Heat Shock Protein 90 (Hsp90) Expression Leads to Increased Apoptosis in the Monoblastoid Cell Line U937 Following Induction with TNF-Alpha and Cycloheximide: A Possible Role for Immunopathology. *J. Immunol.* **1996**, *157*, 4109–4118. https://doi.org/10.4049/jimmunol.1301812.
(28) Thomas, G. P.; Welch, W. J.; Mathews, M. B.; Feramisco, J. R. Molecular and Cellular Effects of Heat-Shock and Related Treatments of Mammalian Tissue-Culture Cells. *Cold Spring Harb. Symp. Quant. Biol.* **1982**, *46* (2), 985–996.
(29) Dulak, J.; Deshane, J.; Jozkowicz, A.; Agarwal, A. Heme Oxygenase-1 and Carbon Monoxide in Vascular Pathobiology: Focus on Angiogenesis. *Circulation*. 2008, pp 231–241. https://doi.org/10.1161/CIRCULATIONAHA.107.698316.
(30) Deshane, J.; Chen, S.; Caballero, S.; Grochot-Przeczek, A.; Was, H.; Li Calzi, S.; Lach, R.; Hock, T. D.; Chen, B.; Hill-Kapturczak, N.; et al. Stromal Cell-Derived Factor 1 Promotes Angiogenesis via a Heme Oxygenase 1-Dependent Mechanism. *J. Exp. Med.* **2007**, *204* (3), 605–618. https://doi.org/10.1084/jem.20061609.
(31) Wang, K.; Wang, X.; Han, C.; Chen, L.; Luo, Y. Scaffold-Supported Transplantation of Islets in the Epididymal Fat Pad of Diabetic Mice. *J. Vis. Exp.* **2017**, No. 125.

https://doi.org/10.3791/54995.
(32) Gibly, R. F.; Zhang, X.; Lowe, W. L.; Shea, L. D. Porous Scaffolds Support Extrahepatic Human Islet Transplantation, Engraftment, and Function in Mice. *Cell Transplant.* **2013**, *22* (5), 811–819. https://doi.org/10.3727/096368912X636966.
(33) Lacy, P. E.; Hegre, O. D.; Gerasimidi-Vazeou, A.; Gentile, F. T.; Dionne, K. E. Maintenance of Normoglycemia in Diabetic Mice by Subcutaneous Xenografts of Encapsulated Islets. *Science (80-.).* **1991**, *254* (5039), 1782–1784. https://doi.org/10.1126/science.1763328.
(34) Smink, A. M.; Li, S.; Swart, D. H.; Hertsig, D. T.; de Haan, B. J.; Kamps, J. A. A. M.; Schwab, L.; van Apeldoorn, A. A.; de Koning, E.; Faas, M. M.; et al. Stimulation of Vascularization of a Subcutaneous Scaffold Applicable for Pancreatic Islet-Transplantation Enhances Immediate Post-Transplant Islet Graft Function but Not Long-Term Normoglycemia. *J. Biomed. Mater. Res. - Part A* **2017**, *105* (9), 2533–2542. https://doi.org/10.1002/jbm.a.36101.
(35) Otto, G. P.; Rathkolb, B.; Oestereicher, M. A.; Lengger, C. J.; Moerth, C.; Micklich, K.; Fuchs, H.; Gailus-Durner, V.; Wolf, E.; Hrabě de Angelis, M. Clinical Chemistry Reference Intervals for C57BL/6J, C57BL/6N, and C3HeB/FeJ Mice (Mus Musculus). *J. Am. Assoc. Lab. Anim. Sci.* **2016**, *55* (4), 375–386.
(36) Boehm, O.; Zur, B.; Koch, A.; Tran, N.; Freyenhagen, R.; Hartmann, M.; Zacharowski, K. Clinical Chemistry Reference Database for Wistar Rats and C57/BL6 Mice. *Biol. Chem.* **2007**, *388* (5), 547–554. https://doi.org/10.1515/BC.2007.061.